Griffiths phase, metal-insulator transition, and magnetoresistance of doped manganites

V. N. Krivoruchko,[1] M. A. Marchenko,[1] and Y. Melikhov[2]
[1]*Donetsk Physics & Technology Institute, NAS of Ukraine, Str. R. Luxemburg 72, 83114 Donetsk, Ukraine*
[2]*Cardiff University, Newport Road, Cardiff, CF24 3AA Wales, United Kingdom*
(Received 11 January 2010; revised manuscript received 12 May 2010; published 18 August 2010)

A phenomenological model is developed for systematic study of the universal features in metal-insulator transition and magnetoresistivity of mixed-phase manganites. The approach is based on utilization of some hypothesis appropriate to the Preisach picture of the magnetization process for half-metallic ferromagnets and an assumption that in doped manganites a Griffiths-type phase exists just above the magnetic-ordering temperature. Within the model, the system is considered as a random three-dimensional resistor network where a self-consistent formation of paths with metal and polaron types of conductivity is not only due to magnetic field variation but also due to temperature changes, as well. Both mechanisms of intrinsic percolation transition are considered on one basis. The theory is able to replicate the basic regularities found experimentally for doped manganites resistivity dependence on temperature and magnetic field without the need for empirical input from the magnetoresistive data. Within the approach a natural basis has arisen for a qualitative classification of magnetoresistive materials into those, such as $La_{0.7}Sr_{0.3}MnO_3$, showing modest magnetoresistivity, and those, such as $La_{0.7}Ca_{0.3}MnO_3$, showing large magnetoresistivity.

DOI: 10.1103/PhysRevB.82.064419 PACS number(s): 75.40.Cx, 75.47.Gk

I. INTRODUCTION

The intrinsic transport properties of doped manganites with the general formula $Ln_{1-x}B_xMnO_3$ (where *Ln* is a lanthanide and *B* is a divalent alkaline earth) having the effect of "colossal magnetoresistance" (CMR)—an abnormal decrease in resistivity when a magnetic field is applied—are far from trivial, and, in fact, have proven to be a challenge to describe.[1–4] While the parent compound $LnMnO_3$ is known to be an antiferromagnetic insulator, the doped compounds in the optimal regime $(Ln^{3+}_{0.7}B^{2+}_{0.3})MnO_3$ behave as paramagnetic (PM) with polaron type of conductivity at high temperatures and ferromagnetic (FM) metals below the Curie temperature T_C, near which the magnetoresistance peaks. The FM ordering has been attributed to the double-exchange interaction between the valence electronic states of Mn^{3+}-O^2-Mn^{4+}.[5] The double-exchange mechanism is also believed to be responsible for the occurrence of CMR in conjunction with the effects of lattice distortion.[6] A direct consequence of the double-exchange and the lattice distortion is a large spin splitting of the conduction band into majority and minority subbands in the FM state.[1–4] These subbands are separated by the on-site Hund's rule energy, which is about several electron volts, depending on the *A*-site doping. The large spin splitting yields the half-metallic properties of the material, namely, at the Fermi level only the states of charge carriers with one spin direction are present whereas there is a gap in the density of states for the carriers with the another spin direction.

Within the double-exchange interaction model, the itinerant charge carriers provide both the magnetic interaction between nearest Mn^{3+}-Mn^{4+} ions and the system's electrical conductivity. Due to the short mean free path, that is typically the distance of about a lattice parameter, the charge carrier probes the magnetization on a very short length scale. So, as a specific prediction of the double-exchange model is that the onset of metallicity reflects the establishment of an infinite (percolating) pathway of metallic bonds and simultaneously the establishment of an infinite ferromagnetic cluster. As a result, a strong interplay between magnetic order and macroscopic electrical resistance is expected.

Indeed, in hole-doped manganites the insulator-to-metal transition is observed just after the ferromagnetic ordering;[1–4] magnetoresistive experiments often exhibit an intricate interplay with magnetization and with the role of field history in the preparation of the system; often a scaling $\rho/\rho_0=-C(M/M_S)^2$ is found between the reduced resistivity, ρ/ρ_0, magnetization, (M/M_S),[2,4,7–10] etc.

There are also numerous evidences proving the spatial variations in the local electronic properties on a nanometer scale and demonstrating the coexistence of metallic, insulating, as well as semiconducting regions, even in state-of-art materials.[1–4,11] While these regions have typical sizes of tens nanometer, they can also form clusters of several hundred nanometers. As was documented in noise measurements,[12] muon spin relaxation[13] and in neutron-scattering experiments,[14] this phase separation is *dynamic*, but much slower than it is typical for critical fluctuations. By applying magnetic field, a considerable fraction of semiconducting regions can be converted into metallic regions, resulting in metallic percolation paths throughout the sample. Despite the fact that, with increasing magnetization, the system becomes increasingly metallic, some regions remain insulating/semiconducting even in a high applied field.[11] Data obtained from high-quality single crystals show almost exclusively semiconducting (polaronic) behavior at temperature far above the Curie temperature. On lowering the temperature, the system becomes more metallic on average, however, there are always regions that remain insulating down to low temperatures far into the bulk ferromagnetic state.

Typically, the zero-field resistivity $\rho(T)$ increases substantially upon cooling, reaches the maximum and then sharply decreases upon further cooling. The temperature at which $\rho(T)$ achieves maximum commonly is considered as insulator-to-metal transition temperature T_{MI}. It was de-

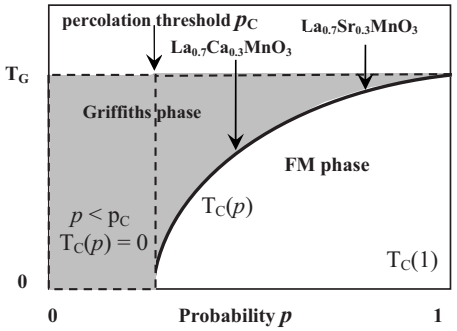

FIG. 1. Presumptive T-p diagram for a dilute ferromagnetic Ising model (Ref. 26); here p is the probability for the existence of a ferromagnetic bond, solid curve is a probable behavior of the Curie temperature $T_C(p)$ of a dilute ferromagnet. A conjectured position of $La_{0.7}Sr_{0.3}MnO_3$ with $T_C(p) \approx 370$ K and $La_{0.7}Ca_{0.3}MnO_3$ with $T_C(p) \approx 220$ K on T-p diagram is shown.

tected, that as the average ionic size of A-site atoms decreases toward that of La, the transition temperature T_{MI} (and the Curie temperature T_C) decreases and the exponential increase in resistivity with temperature makes the drop to metallic resistivity more dramatic.[15–18] Exemplarily, magnetoresistive manganites with high T_C (e.g., $La_{0.7}Sr_{0.3}MnO_3$ with $T_C \approx 350-370$ K) show modest magnetoresistivity and conventional critical behavior whereas those with low T_C (e.g., $La_{0.7}Ca_{0.3}MnO_3$ with $T_C \approx 220$ K) show larger magnetoresistivity and unconventional critical behavior. Because the double-exchange model alone is not sufficient to explain the extraordinary magnitude of magnetoresistance in manganites,[1–4] researchers are forced to look for other scenarios of the metal-insulator transition in manganites.

Recently, a considerable influence of quenched disorder on the phase complexity in manganite systems and the appearance of phenomena such as CMR has been unraveled both experimentally[11,19–23] and theoretically.[24,25] Within the context of quenched disorder scenarios, the existence of a Griffiths-type[26] temperature T_G above the magnetic-ordering temperature T_C has been predicted and linked to CMR.[19,20,25] Below T_G, the disordered system is in between the completely disordered PM high-temperature regime and the magnetically ordered state. This phase regime is usually referred to as the Griffiths phase,[22,23,25,27] based on Griffiths' treatment of the effects of quenched randomness on the magnetization of a dilute ferromagnet.[26] Griffiths phase is microscopically characterized by a clusterlike system induced by disorder. Griffiths showed that essential singularities would develop in a temperature region $T_C(p) < T < T_G$, where p denotes the disorder parameter, $T_C(p)$ is the disorder-dependent FM ordering temperature, and T_G is a new temperature scale corresponding to the Curie temperature of the undiluted system (see Fig. 1).

Almost all the reports considering the Griffiths model are devoted to the *singular* behavior of thermodynamic or dynamic properties of the system.[19,20,22,23,28] To our best knowledge, there were no reports addressing "conventional" (nonsingular) characteristics of the system with Griffiths phase. On the other hand, as far as the disorder effects are an intrinsic part of the physics of manganites, the model considering magnetoresistive properties of these materials in ferromagnetic and Griffiths phases on a single footing is very desirable.

The present study attempts to address these questions by generalizing the effective medium approach[29] assuming the existence of a Griffiths-type phase and temperature scale T_G above the magnetic-ordering temperature. We will show that with an inclusion of the necessary temperature effects the model[29] is able to replicate a broad spectrum of behavior observed experimentally in the field-temperature dependences of the conductivity response of magnetoresistive manganites. In particular, a qualitative classification of magnetoresistive manganites has appeared. Namely, depending on some system parameter, which describes the response of a magnetic system on thermal effects, magnetoresistance will be large, the temperature of insulator-to-metal transition is far below T_G, and the effect of magnetic field is dramatic. Or, oppositely, magnetoresistance will be low, T_{MI} is not far below T_G, and the effect of magnetic field is moderate. We stress that we will not discuss any specific regimes or a class of effects from the diversity of phenomena in doped manganites (reviews[1–4] give a good idea of these), but try to focus on common behavior and basic characteristics of metal-insulator transition and magnetoresistive properties of these materials. The list of universal regularities found for doped manganites includes, in particular, the following: (i) a system with the largest Curie temperature demonstrates modest magnetoresistivity whereas a system with the lowest Curie temperature shows the largest magnetoresistivity; (ii) approximately an inverse relationship between MR effect magnitude and T_C (or T_{MI}) is observed; and (iii) above the Curie temperature there is an exponential resistivity-magnetization relation $\rho(M)/\rho(0) \sim \exp[-C(M/M_S)^2]$. The discussion of these basic characteristics is the main purpose of the report. The analysis necessarily involves phenomenological consideration since aforementioned features, most probably, cannot be discussed within one microscopic model framework. Also, any microscopic theory to be classic should contain everything what is "required" and nothing what is "excess." A correct phenomenological theory helps to sort out what is required and what is excess.

The paper is organized as follows. In Sec. II, to make the report self-contained, we briefly discuss the Preisach model of magnetization, which includes the effects of the critical ordering temperature and thermal fluctuations. Section III describes the modeling of the metal-insulator transition and magnetoresistivity in half-metallic ferromagnets (HMFs) based on the Preisach-approach philosophy. In Sec. IV, the model's predictions of HMF electrical resistivity response on temperature and magnetic field are illustrated by numerical simulations. The results are compared with the experimental data. The next section is devoted to a comprehensive discussion of the approximations made and possible generalizations of the model. We end with the summary.

II. PREISACH-BASED DESCRIPTION OF THE MAGNETIZATION PROCESS

As was already mentioned, systematic studies on the resistivity-magnetization relation in doped manganites below

and above the Curie temperature reveal a surprisingly strong interplay between transport and magnetism in this system. A model which predicts direct relationships between magnetization $M(H,T)$ and magnetoresistivity $R(H,T)$ was recently proposed in Ref. 29. The model is based on utilization of some hypothesis appropriate to the Preisach picture of magnetization process which we briefly discuss in this section.

The classical Preisach model[30,31] assumes that the system consists of a large number of elementary interacting units. Each unit is described by an elementary rectangular hysteresis loop, which has two field parameters, i.e., switching fields, h_A and h_B, $h_A \geq h_B$. A probability distribution function $P(h_A,h_B)$ of the elementary units with switching fields h_A, h_B is assumed to be known. Under varying external magnetic field H, the unit will switch its magnetization to the "up" state, if external field increases to $H \geq h_A$; the unit will switch to the "down" state, if external field decreases to $H \leq h_B$. However, the magnetization will depend on the previous history of changes, if external magnetic field is in the region: $h_A \geq H \geq h_B$. The magnetization may be calculated knowing the history of variation in the magnetic field, which generates a partition of the Preisach plane (h_A,h_B) into two regions with only up or down hysterons state

$$M(H) = \mu_s \int \int_{S^{(+)}} P(h_A,h_B) dh_A dh_B - \mu_s \int \int_{S^{(-)}} P(h_A,h_B) dh_A dh_B,$$

where all elementary units in the region $S^{(+)}$ have the magnetization "$+\mu_s$," all units in the region $S^{(-)}$ have the magnetization "$-\mu_s$." It is convenient to introduce the new field coordinates $h_c=(h_A-h_B)/2$ and $h_u=(h_A+h_B)/2$, and rewrite this expression in the form

$$M(H) = 2\mu_s \int_0^{\infty} dh_c \int_0^{b(h_c)} dh_u P(h_c,h_u),$$

where the (non-negative) Preisach distribution function $P(h_c,h_u)$ has been suitably renormalized to include all unimportant numerical factors. The boundary line $b(h_c)$ represents the staircase boundary between the $S^{(+)}$ and $S^{(-)}$ regions and comprises a given external field history.

One of the remarkable features of the Preisach-based approach is that it yields joint description of hysteresis and thermal-fluctuation effects.[31–33] Indeed, transitions between the two states of hysteron may also be induced by thermal fluctuations if the system is at a finite temperature T. For an experiment with a characteristic time parameter $t_{\rm exp}$, thermal transitions are bounded to those barriers which are less or equal to the effective thermal-fluctuation energy $W_{fl}(T) = k_B T \ln(t_{\rm exp}/\tau_0)$.[31,34] Here k_B is Boltzmann's constant; τ_0 is a typical attempt time on the order of 10^{-9}–10^{-10} s. The time parameter $\ln(t_{\rm exp}/\tau_0)=25$ is typical for static experimental measurements.

As was demonstrated by Song *et al.*[32] (see also Ref. 33), the field and thermal excitation conditions can be represented graphically in the Preisach plane, in which each hysteron is located with respect to its characteristic fields (h_c,h_u). Figure 2 shows the Preisach plane in a positive applied field $H>0$ at finite temperature T. The quadrant enclosed between the boundaries $h_u=H+h_c$ and $h_u=H-h_c$ contains the bistable subsystems, which can potentially occupy either state $\pm\mu(T)$. For a given temperature T, there are two thermal-excitation boundaries; one of which—$h_{T\ min}$—identifies those subsystems whose lower energy barrier matches $W_{Tl}(T)=\mu(h_c-|h_u+H|)$, and the other one—$h_{T\ max}$—is the location of subsystems whose higher barrier matches $W_{Th}(T)=\mu(h_c+|h_u+H|)$. Subsystems which lie to the left or above the $h_{T\ min}$ boundaries have a thermally active lower barrier and a thermally inactive higher barrier, and consequently occupy their lower energy state exclusively, while those subsystems within the shaded region in Fig. 2 have two thermally active barriers, equilibrium Boltzmann level populations and a superparamagnetic response function $\mu_{sp}(H,T)=\mu(T)\tanh[\mu(T)(H-h_u)/k_BT]$. Now the magnetization is obtained by evaluating the weighting state $\varphi(H,T,h_c,h_u)$ of each hysteron by the Preisach function $P(h_c,h_u)$ and integrating over the entire Preisach plane

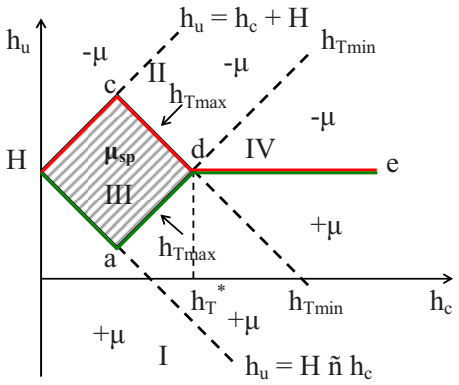

FIG. 2. (Color online) The Preisach plane in a positive applied field $H>0$ at finite temperature T. The region of superparamagnetic response is hatched; in this region hysterons can potentially occupy either of $\pm\mu(T)$ state. In the region IV the response is history dependent (see text for details).

$$M(H,T) = \int_0^{\infty} dh_c \int_{-\infty}^{\infty} [dh_u P(h_c,h_u) \varphi(H,T,h_c,h_u)] \quad (1)$$

with

$$\varphi(H,T,h_c,h_u) = \{+\mu(T), -\mu(T), \mu(T) \times \tanh[\mu(T)(H-h_u)/k_BT], \pm\mu(T)\}$$

for the regions I, II, III, and IV in the Preisach plane, respectively (see Fig. 2). In the region IV, where hysterons can potentially occupy either of $\pm\mu(T)$ state, the response is history dependent and is determined by the line $b(h_c)$.

According to the Preisach-approach paradigm the distribution function $P(h_c,h_u)$ is an inherent property of the system which is prescribed in advance. Typically[31] it is assumed that there is no interference between local coercivity and interaction effects and the Preisach distribution function may be split into the product of factors. A Gaussian-Gaussian distribution of the form

$$P(h_c,h_u) = (2\pi\Lambda_c^2)^{-1/2}\exp\left[-\frac{(h_c-h_{c0})^2}{2\Lambda_c^2}\right](2\pi\Lambda_u^2)^{-1/2} \times\exp\left[-\frac{h_u^2}{2\Lambda_u^2}\right] \quad (2)$$

is often a good approximation. Here h_{c0}, Λ_c, and Λ_u are distribution parameters. Temperature dependence of the hysterons energy barriers is described by introducing temperature dependences into the Preisach function parameters (exact relationships will be introduced below, also see Ref. 32 for details).

III. CORRELATION BETWEEN RESISTIVE AND MAGNETIC STATES IN HALF-METALLIC FERROMAGNETS

Consider now the system under study as a system of magnetic hysterons distributed in real space.[29] Let us decompose a total current through the sample into two spin-polarized currents (two-fluids model) $j_{total}=j_\uparrow+j_\downarrow$, where, due to half-metallic properties of the material, $j_\uparrow$ can be considered as a current through one type (+) of the Preisach hysterons (units) while $j_\downarrow$ as a current through another (−) type of the units. At zero temperature, the electron-spin direction is parallel to the magnetic moment of the initial hysteron and may be parallel or antiparallel to the direction of the magnetic moment of the nearest-neighbor hysterons. If parallel, the electron experiences weak scattering and hence that is a "metallic path." If antiparallel, the electron experiences strong scattering and hence high resistance occurs (a "resistive path"). Therefore, the system can be represented as three-dimensional resistor networks. When the hysteresis is rate independent, the system's conductivity is obtained by weighting the conductivity of each resistor network path by the Preisach conductivity function, $P(h_{Ai},h_{Bi},\ldots,h_{Ai+k},h_{Bi+k})$. As a result, we obtain the following expression for an irreversible conductivity:[29]

$$\sigma_{irr}(H) = \sum_{k=1}^{\infty}\int\int_{b(h_c)} dh_{Ai}dh_{Bi}\ldots\int\int_{b(h_c)} dh_{Ai+k}dh_{Bi+k} \times P(h_{Ai},h_{Bi},\ldots,h_{Ai+k},h_{Bi+k}) \times\sigma(H;h_{Ai},h_{Bi},\ldots,h_{Ai+k},h_{Bi+k}), \quad (3)$$

where $b(h_c)$ is the Preisach memory function, the same as for magnetic hysteresis. The correlation between magnetic and resistivity responses has now become a correlation between the Preisach magnetic function, $P(h_A,h_B)$, and the Preisach conductivity function, $P(h_{Ai},h_{Bi},\ldots,h_{Ai+k},h_{Bi+k})$.

For hole-doped manganites, due to the short spin scattering length, the charge carrier probes the magnetization on a very short (atomic) length scale. So, as a good approximation we can assume that there are no mutual interference of neighboring hysterons on their switching fields, h_A and h_B. That is, the Preisach conductivity function $P(h_{Ai},h_{Bi},\ldots,h_{Ai+k},h_{Bi+k})$ may be represented as a multiple function of the probability $P(h_A,h_B)$ of magnetic hysteron being involved in a conducting path

$$P(h_{Ai},h_{Bi},h_{Ai+1},h_{Bi+1}) = c_1P(h_{Ai},h_{Bi})P(h_{Ai+1},h_{Bi+1}),$$

$$P(h_{Ai},h_{Bi},h_{Ai+1},h_{Bi+1},h_{Ai+2},h_{Bi+2}) = c_2P(h_{Ai},h_{Bi})P(h_{Ai+1},h_{Bi+1})P(h_{Ai+2},h_{Bi+2}), \quad (4)$$

and so on. For the given current trajectory, any mutual permutations of the hysterons are physically indistinguishable and have to be taken into account once, i.e., $c_k=\text{const}/k!$, where "const" is determined by the distribution of the hysterons in a given sample. It may be considered as the probability of two hysterons with switching fields (h_{Ai},h_{Bi}) and (h_{Ai+1},h_{Bi+1}) to be the nearest neighbors in real space[29] and reflects the character of a quenched disorder in the given sample. It is reasonable to assume that this probability does not depend on temperature and magnetic field and is an inherent property of the system.

We are now in a position to generalize the results of Ref. 29 by including the temperature effects. First of all, we should determine the temperature dependence of the hysterons energy barriers and the Preisach function parameters. Following the picture of the quenched disorder and the existence of a Griffiths-type temperature scale T_G,[11,19,21,23,24] we will suggest the ratio T/T_G as a natural scale for the temperature dependence of the system parameters. Within a qualitative approach (see also the Sec. V), power-law temperature dependences has been considered

$$h_{c0}(T) = h_{c0}\left(1-\frac{T}{T_G}\right)^{\gamma_h},\quad \Lambda_c(T) = \Lambda_{c0}\left(1-\frac{T}{T_G}\right)^{\gamma_c},\quad \Lambda_u(T) = \Lambda_{u0}\left(1-\frac{T}{T_G}\right)^{\gamma_u},\quad \mu(T) = \mu_s\left(1-\frac{T}{T_G}\right)^{\gamma_M}, \quad (5)$$

where γ_h, γ_c, γ_u, and γ_M are critical exponents and μ_s is magnetization of hysteron at zero temperature (note, that the notations used here differ slightly from those introduced by Song *et al.*[32] to avoid confusion).

For later purposes, it is also convenient to introduce characteristic energies, which form a natural basis for a qualitative classification of magnetic system response on thermal effects. One of these characteristic energies is the critical thermal-fluctuation energy $W_{Cfl}=k_BT_G\ln(t_{\exp}/\tau_0)$, which defines the highest energy barrier which can be thermally activated for a hypothetical "pure") system with "Curie temperature" T_G. The other one is the mean zero-temperature anisotropy barrier $W_A(0)=\mu_sh_{c0}$, which fixes an upper limit on the height to which the barriers of a given system can grow. The relation of these two characteristic energies, $\eta=W_A(0)/W_{Cfl}$, determines the ability of a system to resist thermal-fluctuations effects. For the system with $\eta<1$, thermal energy is sufficient to activate almost all of the barriers, so this system will mainly exhibit a reversible superparamagnetic response. Following[32] we will refer to such a system as the fluctuation-dominated system. Oppositely, the system with $\eta>1$ will mainly exhibit an irreversible response and the superparamagnetic behavior will be narrow. We will refer to such a system as the anisotropy-dominated system. As will be shown below, a ratio of the characteristic energies $W_A(0)$ and W_{Cfl} is a natural parameter for classification of HMF systems in terms of their magnetoresistive properties. The main idea introduced here is that certain fundamental characteristic energies which play a primary role in the metal-to-

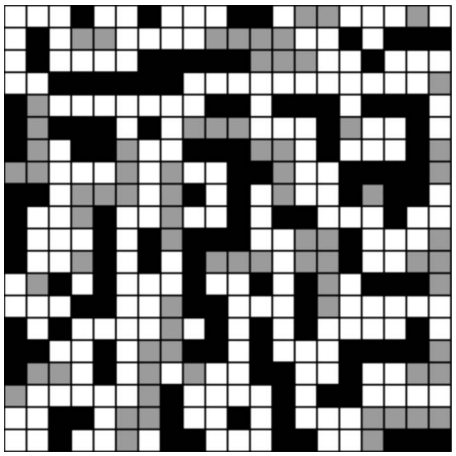

FIG. 3. An example of magnetic hysterons distribution in real space at finite temperature. Here the squares of different colors represent the hysterons in spin up (black), spin down (white), or superparamagnetic (gray) state. The picture imitates a local variation in the electronic properties of mixed-phase manganites.

insulator transition and magnetoresistive properties of the system are determined by the energy barriers alike to those that are for a hypothetical system with the Curie temperature T_G.

As was stated before, three-dimensional resistor networks were introduced to describe the transport properties. At finite temperature, however, these networks are composed of hysterons which can potentially occupy *three* states. Figure 3 schematically illustrates a system of magnetic hysterons distributed in real space at finite temperature. Here the squares of different color represent hysterons with the magnetization up (black), magnetization down (white), and hysterons in superparamagnetic state (gray). The main concept introduced is that the percolation process is not only due to magnetic field variation but also due to temperature changes as well. Our approach implies that (i) the metallic state reached from the insulator with *magnetic field increase* is not homogenous but must have a substantial fraction of insulating clusters and (ii) the metallic clusters exist in the range $T_{MI} \leq T \leq T_G$. Accordingly, this also suggests that the metallic state reached from the insulator with *temperature decrease* is not homogeneous and even below T_{MI} there is a substantial fraction of the insulating (paramagnetic) clusters. The metal-to-insulator transition is associated with the formation of a metallic cluster that spans the entire sample. Further increase in conductivity is likewise understood as the growth of such a cluster.

The physics sketched in Fig. 3 gives possibility to model the real situation observed experimentally for mixed-phase ferromagnetic manganites (cf. with Fig. 3 in Ref. 11). As documented in different experiments, even in perfect single crystals there is local variation in the electronic properties and spatial coexistence of metallic, insulating, and semiconducting regions—the so-called phase separation. Taking into account the data, one can consider the sample as an ensemble of physically small but finite (e.g., a few nanometers in size) "particles" (hysterons). Then each point of the Preisach plane represents the average behavior of a certain group of real particles in the medium. Conductivity between two neighboring hysterons depends on many factors. In order to clarify how magnetic percolation determines the transport properties of the system, the dependence of charge-carrier transport on the relative orientation (parallel, antiparallel, or superparamagnetic) of magnetic moments of the neighboring hysterons will be considered. Following the description presented above for zero temperature, if overall orientations are parallel then the electron will be in a "conductive state" (metallic). If antiparallel, the electron will be in a "resistive state" (insulating). Intermediate case for conductivity will be if one or two of the neighboring hysterons are in the superparamagnetic state (such cases will be called polaron). Finally, as in the case for zero temperature, the system's conductivity is obtained by weighting the conductivity of each resistor network path by the Preisach conductivity function, $P(h_{Ai}, h_{Bi}, \ldots, h_{Ai+k}, h_{Bi+k})$ with temperature dependence. As was already noted, this approach is very reasonable for doped manganites, where it is known that electron scattering drastically depends on electron-spin direction.

The irreversible part of the conductivity is obtained by evaluating the weighting state of the conductivity of hysteron pairs in Eq. (3), which is now temperature-dependent function $\sigma(H,T;h_{Ai}, h_{Bi}, \ldots, h_{Ai+k}, h_{Bi+k})$, by the Preisach conductivity function with temperature-dependent parameters, and integrating over the entire Preisach plane. In the general case, all possible current trajectories through magnetic hysterons should be taken into account [for $T=0$ see Eq. (3) in Ref. 29]. However, the analysis shows that even the first approximation of a single pair of adjacent domains (hysterons) is a good approximation to the main part of experimental data. The physical background for this may be a random potential arising in doped manganites from chemical disorder in the conventional random alloying on the perovskites A-site with rare-earth and alkaline-earth ions (see, e.g., Ref. 21 for more details), which suppresses the respective long-range hysterons correlations. Different lattice distortions also provide an additional natural mechanism for short-range correlation in the material.[35] Leaving the general case for future consideration, here we consider the first nontrivial approximation, i.e., the magnetoresistance is mainly associated with the mutual orientation of magnetization of neighboring hysterons. Then Eq. (3) can be transformed into

$$\sigma_{irr}(H,T) = \int\int_{b(h_c)} dh_{ci}dh_{ui} \int\int_{b(h_c)} dh_{ci+1}dh_{ui+1} \times P(h_{ci},h_{ui})P(h_{ci+1},h_{ui+1}) \times \sigma(H,T;h_{ci},h_{ui},h_{ci+1},h_{ui+1}). \quad (6)$$

Here we used the relation Eq. (4) and rewrote the result in field coordinates h_c and h_u and introduced temperature dependence in Preisach function and conductivity. Equation (6), in the limiting case of ignoring the temperature effects and using Eq. (1), reproduces the results of Refs. 7, 8, and 29

$$\sigma_{irr}(H)/\sigma_0 \sim \left[\int\int_{b(h_c)} dh_c dh_u P(h_c,h_u)\varphi(H;h_c,h_u)\right]^2 \sim [M(H)/M_s]^2, \quad (7)$$

where σ_0 is a conductivity at $T=0$.

By decomposing the integrals in Eq. (6) into integrals over regions I, II, III, and IV in the Preisach plane (see Fig. 2), we can present the conductivity $\sigma_{irr}(H,T)$ as a sum of partial conductivities through the paths with the given type of hysteron pairs resistivity state

$$\sigma_{irr}(H,T) = \sum_{i,j=I}^{IV} \sigma_{i,j}(T) V_{i,j}^{(R)}(H,T) \tag{8}$$

which, after combining terms with the same meaning, can be rewritten as

$$\sigma_{irr}(H,T) = \sigma_m(T) V_m^{(R)}(H,T) + \sigma_{sp}(T) V_{sp}^{(R)}(H,T) + \sigma_I(T) V_I^{(R)} \times (H,T), \tag{9}$$

where $V_m^{(R)}(H,T)$ stands for the volume fraction of a metallic conductivity path, $V_{sp}^{(R)}(H,T)$ is the volume fraction of the sample with a polaron-type conductivity (due to superparamagnetic region on the Preisach plane), and $V_I^{(R)}(H,T)$ corresponds to volume fraction of hysteron pairs with mutual antiparallel magnetization orientations, and H dependence represents dependence of history of magnetic field variation. Each volume fraction is just proportional to that of region on the entire Preisach plane. The $\sigma_{m(sp,I)}(T)$ is the conductivity of a metallic (polaron, insulating) conductivity path, respectively. We assume that none of these parameters and parameter $\sigma_{rev}(T)$ (see below) depends on magnetic field. A conductivity of the adjacent hysterons which form an "insulating" path will equal zero $\sigma_I(T)=0$. These are certainly simplifications but we will show below that even such a simplified model is still able to give a good qualitative description of the main experimental facts for temperature—field-resistivity behavior of doped manganites.

For comparison with real systems it is necessary to supplement irreversible response by a purely reversible term $\sigma_{rev}(T)$ which represents processes independent of magnetic state of the system, i.e., $\sigma_{tot}(H,T)=\sigma_{rev}(T)+\sigma_{irr}(H,T)$. [The $\sigma_{rev}(T)$ characterizes a high-temperature asymptotic of the conductivity.] We will assume, again for simplicity, that the reversible term is due to a polaron mechanism of conductivity, too, and that the characteristic parameters of the polaron transport do not change, i.e., $\sigma_{rev}(T)=\sigma_{sp}(T)$.[36] The total conductivity is given then by the expression

$$\sigma_{tot}(H,T) = \sigma_m(T) V_m^{(R)}(H,T) + \sigma_{sp}(T)[1 - V_m^{(R)}(H,T)], \tag{10}$$

where the volume fraction with metallic type transport is just proportional to that of region on the entire Preisach plane. Namely,

$$V_m^{(R)}(H,T) = \left[\mu(T)/\mu_s \int_0^{\infty} dh_c \int_{-\infty}^{b_1(h_c)} dh_u P(h_c,h_u) \right]^2 + \left[-\mu(T)/\mu_s \int_0^{\infty} dh_c \int_{b_2(h_c)}^{\infty} dh_u P(h_c,h_u) \right]^2, \tag{11}$$

where the boundary $b_1(h_c)$ (line H-a-d-e in Fig. 2) separates the region where hysterons occupy state $+\mu(T)$ while the boundary $b_2(h_c)$ (line H-c-d-e in Fig. 2) separates the region were hysterons occupy state $-\mu(T)$.

To proceed further, we need to specify for the dependence of the conductivities $\sigma_m(T)$ and $\sigma_{sp}(T)$ on temperature. These dependences on temperature are determined by the microscopic mechanisms of charge-carriers scattering specific for a system and are the matter of a microscopic theory consideration. Within our phenomenological approach, we will use here the known experimental results. In a metallic regime, for such HMFs as manganites electrical resistivity is found to obey the following relation (see, e.g., Ref. 37):

$$\rho_{dc}(T) = \rho_0 + \rho_{ee}T^2 + \rho_{em}T^{9/2} = \sigma_0^{-1}(1 + \alpha T^2 + \gamma T^{9/2}) = \sigma_m^{-1}(T), \tag{12}$$

where $\rho_0=\rho_{dc}(T=0,\ H=0)=1/\sigma_0$ is the residual resistivity arising from temperature-independent processes such as impurities, vacancies, etc. The term $\sim T^2$ represents the electron-electron scattering whereas the term $\sim T^{9/2}$ stands for the two-magnon scattering process in ferromagnetic phase.[38] (Note that for HMFs the one-magnon scattering process in ferromagnetic phase is forbidden.) Numerous experiments show that at low temperature the metallic region's resistivity of manganites is mainly governed by the electron-electron scattering while the contribution of the two-magnon scattering process is more important at high temperatures.

A number of experimental results including transport measurements,[9,39] isotope effects,[40] and microscopic techniques[41] have provided strong evidence to the (small or large) polaron-type conductivity in the paramagnetic region. In the framework of the hopping of small polarons model the electrical resistivity can be expressed as:[42] $\rho(T) = \rho_0 T^n \exp(E_p/k_BT)$, where E_p is the sum of the activation energy required for the creation and activation of the hopping of the carries (for manganites, typically $\sim 2k_BT_{MI}-3k_BT_{MI}$), n is 1 for adiabatic and 1.5 for nonadiabatic processes. Experimental data exhibit an independence of the activation energy E_p on magnetic field in paramagnetic region. Within a comparative approach (see also Sec. V), we will approximate the conductivity of neighboring hysterons which are both in the superparamagnetic state, as well as if only one of the neighboring hysterons is in the superparamagnetic state, by the form

$$\sigma_{sp}(T) = \sigma_0 T^{-1} \exp(-E_p/k_BT). \tag{13}$$

Expressions in Eqs. (2), (5), and (10)–(13) are the basis for modeling of the magnetotransport properties of the material for all experimental protocols. In obtaining these expressions, a key assumption was that the system effectively is a three-dimensional resistor network of conductivity hysterons and the transport of this effective medium is characterized by a mixing of band-type and polaron-type conductivities. As will be shown in the next section, the model is able to correctly replicate the main universal findings for doped manganites' resistivity on temperature and magnetic field dependencies.

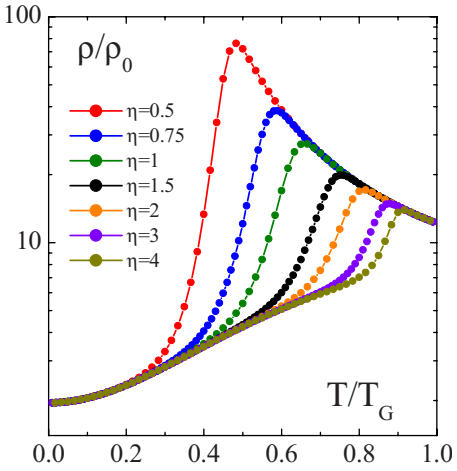

FIG. 4. (Color online) Temperature profiles of resistivity for systems with different $\eta = W_A(0)/W_{Cfl}$ at $H=0$.

IV. RESULTS OF SIMULATION

In this section we present the results of numerical simulations of magnetotransport properties of phase-separated manganites. The parameters used are: $\gamma_c = \gamma_u = \gamma_h = 0.3$, $\gamma = 0.2$, $\gamma_M = 0.5$, $\alpha = 5$, $\Lambda_{c0} = \Lambda_{u0} = 0.35$, $\sigma_0 = 1$, and $E_p/T_G = 2.5$ Oe/emu K. Magnetic field, resistivity, and magnetization are normalized on h_{c0}, ρ_0, and M_S, respectively. We also choose $k_B/\mu_s = 0.08$, 0.053, 0.04, 0.027, 0.02, 0.013, and 0.01 to model the systems with $\eta = W_A(0)/W_{Cfl} = 0.5$, 0.75, 1.0, 1.5, 2.0, 3.0, and 4.0, respectively.

Figure 4 shows the temperature profiles of the resistivity $\rho(T)$ for samples with varying η. T_{MI} is manifested as peak in the $(d\rho/dT)/\rho_0$ curve or as the temperature where $(d\rho/dT)$ changes its sign. As it is apparent, the transition becomes more gradual with increasing η. If magnetic field is applied, the resistivity on temperature dependence is typically measured by the standard field-cooling (FC) protocol. The simulation of field-cooling from a high temperature on the Preisach plane (Fig. 2) corresponds to translation of the vertex $h_c = h_T^*$ inward along the line $h_u = H$ starting from $h_c = h_T^* = \infty$, where the entire bistable quadrant is superparamagnetic. Figure 5 illustrates representative results obtained by such protocol for the fluctuation-dominated $\eta = 0.5$ [Fig. 5(a)] and

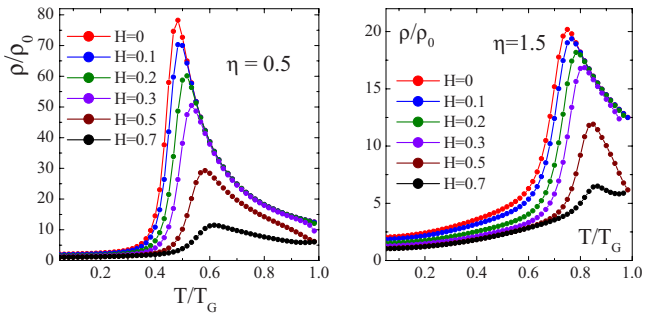

FIG. 5. (Color online) Resistivity data as function of temperature at different applied magnetic fields: (a) fluctuation-dominated system; (b) anisotropy-dominated system. (Here and in Figs. 6, 7, and 9 an external magnetic field is normalized on h_{c0}.)

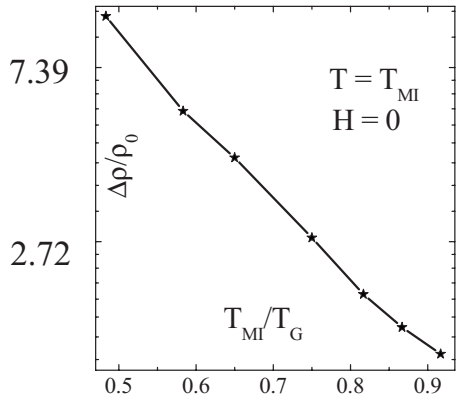

FIG. 6. The variation in the magnetoresistivity, Eq. (14) at $H=0.5$, as function of the ratio T_{MI}/T_G.

anisotropy-dominated $\eta = 1.5$ [Fig. 5(b)] systems.

As it follows from Fig. 5, for both systems at low temperatures the resistivity is metallic, rising sharply while approaching to metal-insulator transition and showing activated (polaron-type) behavior above T_{MI}. Under the effect of magnetic field the T_{MI} is shifted to upper temperature and the magnitude of the resistivity at T_{MI} is decreased. The magnetoresistance is maximal near the metal-insulator transition leading to a peak in the magnetoresistance (MR) ratio

$$\frac{\Delta\rho}{\rho(H)} = -\frac{\rho(T_{MI},H) - \rho(T_{MI},0)}{\rho(T_{MI},H)}. \tag{14}$$

Still, there are some important differences between these two systems. For fluctuation-dominated system [Fig. 5(a)], the resistivity decreases suddenly both below and above T_{MI}, the magnitude of this decrease is large, and the temperature T_{MI} is far below T_G: $T_{MI} \ll T_G$. For anisotropy-dominated systems [Fig. 5(b)], the resistivity decreases much more smoothly both below and above T_{MI}, the magnitude of this decrease is weaker, the effect of magnetic field is moderate, and the T_{MI} is not far below T_G.

The data in Figs. 4 and 5 are in remarkable agreement with the experimental findings for colossal magnetoresistive manganites. It is generally observed that in the doped manganites the transition becomes more smooth and the height of MR peak decreases with increasing the metal-to-insulator transition temperature T_{MI}. The colossal magnetoresistance can be found in compounds with low-T_{MI} temperature; the $La_{0.7}Ca_{0.3}MnO_3$ is the representative of such a system. For the compound with the highest T_{MI} temperature of manganites family, the MR ratio is an order lower; the $La_{0.7}Sr_{0.3}MnO_3$ is the representative of such a system.

Figure 6 shows the results of calculations for the peak of MR, Eq. (14), versus T_{MI}/T_G for a variety of systems with the parameter η ranging from 0.5 to 4.0 at field $H=0.5$. An inverse relationship between T_{MI} and the peak MR is quite visible. The maximum magnetoresistance at a given field appears to be a universal function of the ratio T_{MI}/T_G. Taking into account that in real samples of phase-separated manganites the tunneling percolation mechanism[43] also gives additional contribution into magnetoresistivity, we believe that there is a good qualitative agreement between the prediction

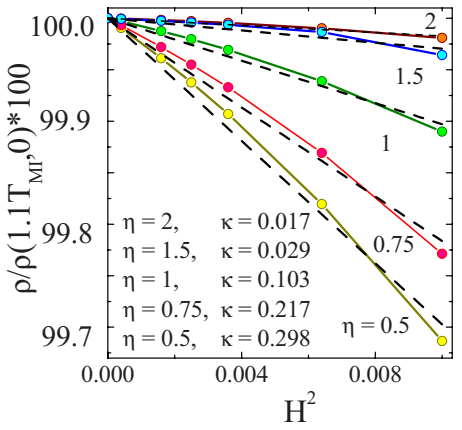

FIG. 7. (Color online) The variation in the normalized resistivity $\rho(H)/\rho(0) \sim \exp(-\kappa H^2)$ as a function of the square of magnetic field at temperature immediately above $T_{MI}(T=1.1T_{MI})$.

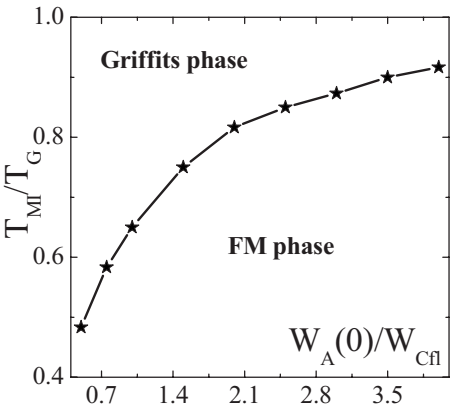

FIG. 8. The variation in T_{MI}/T_G at $H=0$ with parameter $\eta = W_A(0)/W_{Cfl}$, which characterizes the ability of the system to resist thermal fluctuations. (cf. with Fig. 1).

of our simplified model (Fig. 6) and experimental results for the peak MR versus T_C for a variety of $Ln_{1-x}B_xMnO_{3-\delta}$ materials at fields ranging from 5 to 12 T (see the data in Fig. 3 of Ref. 16 or in Fig. 47 of Ref. 1).

Figure 7 illustrates the normalized resistivity $\rho(H)/\rho(0)$ as a function of the square of magnetic field in the temperature region immediately above $T_{MI}(T=1.1T_{MI})$. This dependence was analyzed by using in a paramagnetic state the relation $\rho(H)/\rho(0) \sim \exp[-C(M/M_S)^2] \sim \exp(-\kappa H^2)$ [here $\kappa = C(\chi/M_S)^2$ and χ is dc susceptibility]. As indicated by the broken lines, this empirical formula reproduces well the MR behavior over a fairly large H region. The variation in the coefficient κ with η is shown in inset of Fig. 7. The κ value demonstrates a distinct decrease with increasing the ability of the system to resist thermal fluctuations, i.e., the parameter $W_A(0)/W_{Cfl}$.

The empirical relation $\rho(H)/\rho(0) \sim \exp[-C(M/M_S)^2]$ was originally proposed assuming that the resistivity in a ferromagnetic semiconductor above T_{MI} obeys the thermal-activation-type law, and that the activation energy is reduced in proportion to M^2. Particularly, in Ref. 44 this formula was applied to the MR of low-doped manganites assuming that the mobility edge present within the conduction band shows the energy shift in proportion to M^2. In Ref. 45, the coefficient C is connected with barriers due to magnetic disorder. In Ref. 18, the coefficient C is further related with Curie temperature T_C. Comparing the data in Fig. 7 with those in Fig. 4 of Ref. 18, one can find a remarkable correspondence between the theoretical calculations and experiments.

Generalizing the results in Figs. 4–7, we arrive to the conclusion that the model proposed gives a natural parameter for a qualitative classification of the magnetoresistive manganites. This parameter is the ratio of characteristic energies $W_A(0)/W_{Cfl}$, which are the upper limit on zero-temperature anisotropy barrier $W_A(0)=\mu_s h_{c0}$ and the highest energy barrier which can be thermally activated $W_{Cfl}=k_B T_G \ln(t_{exp}/\tau_0)$. To clarify the physical content of the ratio $W_A(0)/W_{Cfl}$, in Fig. 8 the variation in T_{MI} at $H=0$ with $\eta=W_A(0)/W_{Cfl}$ is shown. We see that the ratio T_{MI}/T_G is increased as η increases. Comparing the T_{MI}/T_G behavior with those suggested for the dependence of $T_C(p)$ on the disorder parameter p (Fig. 1), one can conclude that the parameter $W_A(0)/W_{Cfl}$ realizes function similar to the disorder parameter of the Griffiths model. Following the classification, the model predicts that for the anisotropy-dominated system $(W_A(0)/W_{Cfl}>1)$ the Griffiths-type behavior will be detected in a very narrow region $T_{MI}<T<T_G$; this system will demonstrate modest magnetoresistivity and conventional critical behavior. Oppositely, for the system with dominated temperature fluctuation behavior $(W_A(0)/W_{Cfl}<1)$ the Griffiths region is very broad, and for such a system one can expect large magnetoresistivity and unconventional critical behavior. These qualitative classification is also in a remarkable agreement with the experimental results (see, e.g., Table II in Ref. 20 and Table I in Ref. 28).

Leaving for a forthcoming publication detailed analysis of *magnetic* reversible/irreversible characteristics of a system with the Griffiths phase, let us conclude this section with a brief discussion of those magnetic properties which are directly concerned with the questions under consideration. Figure 9 shows a comparison of the temperature dependence of the FC and zero-field-cooling (ZFC) magnetization response

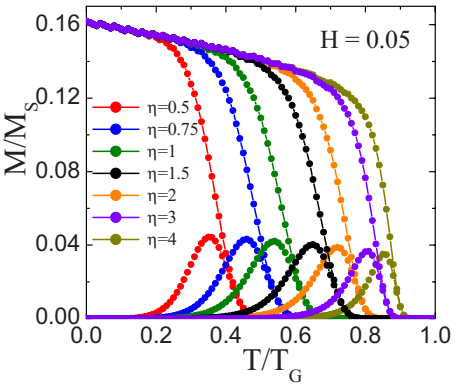

FIG. 9. (Color online) The temperature dependence of the FC and ZFC magnetization responses for a half-metal ferromagnet with the Griffiths phase in an applied field $H=0.05$.

TABLE I. The blocking temperature T_B, the metal-to-insulator transition temperature T_{MI}, and the Curie temperature T_C for systems with different values of the parameter $\eta = W_A(0)/W_{Cfl}$.

η	0.5	0.75	1.0	1.5	2.0	3.0	4.0
T_B	0.43	0.54	0.62	0.72	0.78	0.85	0.89
T_{MI}	0.48	0.59	0.66	0.75	0.81	0.88	0.91
T_C	0.48	0.59	0.66	0.76	0.82	0.88	0.91

$$m(H,T) = M(H,T)\frac{V_m^{(R)}(H,T)}{V_m^{(R)}(H,T=0)} \tag{15}$$

of the fluctuation-dominated ($\eta < 1$) and anisotropy-dominated ($\eta > 1$) systems, in an applied field $H=0.05$. (We take into account that only metallic part of the medium possesses ferromagnetic properties.) From these data one can restore the *actual* Curie temperature T_C and the so-called blocking temperature T_B. The later is the temperature below which the FC and ZFC moments follow different branches, with the FC moment always lying above the ZFC moment, and above which the two branches merge into a single superparamagnetic tail which extends up to T_C. The data for T_C, T_B, as well as T_{MI} are summarized in Table I. From the data in the table, one can find the relation $T_B \leq T_{MI} \leq T_C$ is fulfilled between the temperatures. We will discuss the physical content of the characteristic temperatures relation in the next section.

V. DISCUSSION

Let us now discuss the approximations made and possible generalizations of the model. First of all, we note that our model should be distinguished from those used for describing magnetotransport properties of granular ferromagnetic systems and polycrystalline manganites (see, e.g., Ref. 43 and references therein). The granular system typically is modeled within the tunneling percolation scenario, that is each contact between a pair of grains i and j is represented by a resistor with conductance σ_{ij} proportional to the tunneling probability $\sigma_{ij}=\sigma(\theta_{ij})\exp(-\xi r_{ij})$, where $\sigma(\theta_{ij})$ is a constant of conductivity which is a function of the relative orientation angle θ_{ij} between the magnetic moments of the grains, r_{ij} is the distance between the ith and jth grains, and ξ is a coefficient. Looking for *intrinsic* transport properties of phase-separated manganites we suggested that for an idealized system (e.g., a prefect single crystal) the contribution of a tunneling mechanism into magnetoresistivity does not principally change the results discussed here. This suggestion is closely related to the other one, namely, the idea to use a *scalar* Preisach model. Note, that there are vector versions of the Preisach model (see, e.g., Ref. 46 and references therein), which one can use if further refinements in the approach are needed. But taking into account a good correspondence between the theoretical calculations and experimental data, *a posteriori*, we conclude that vector character of magnetization, as well as angular dependence of the conductivity $\sigma(\theta_{ij})$, are not crucial for the results under consideration. In reality, there is physical justification for these. Indeed, due to the half-metallic nature of electrical transport in the system, conductivity between two neighbor grains (hysterons) strongly depends on the angle between the magnetic moments of the hysterons; specifically, $\sigma(\theta_{ij})$ is very low if the angle θ_{ij} is not near zero value.[43] As already mentioned in Sec. I, in manganites the itinerant charge carriers provide both the magnetic interaction between nearest Mn^{3+}-Mn^{4+} ions (the so-called double-exchange interaction) and the system's electrical conductivity. That is, the charge carrier probes the ions magnetization orientation on a lattice-parameter distance. If the Mn^{3+} and Mn^{4+} core moments are not ferromagnetically ordered the double-exchange interaction is strongly suppressed.[5] Hence, we believe that ignoring an angular dependence of $\sigma(\theta_{ij})$ and the scalar version of our model are not fundamental for the results discussed here.

In our approach, the value of metal and polaron paths is determined by the Preisach distribution function which is the same as for the magnetization. A probability function $P(h_c,h_u)$ is a given characteristic of the sample, which is attributed to the sample solely. The $P(h_c,h_u)$ function can be *independently* restored from magnetization measurements for some definite protocols. For example, following the way as described in Ref. 47, see also Eq. (1), we have

$$P(h_c,h_u) = -\frac{\partial^2}{\partial h_c\,\partial h_u}M(h_c,h_u), \tag{16}$$

where $h_c > h_u$ (see Ref. 47 for more details). That is, all *magnetic parameters* of the system, including their temperature dependences could be restored from the magnetization measurements only. With the probability function $P(h_c,h_u)$ in hands one can then restore the $\rho(T,H)$ dependencies and compare the theoretical curves with those experimentally detected for the given sample. By choosing a power-law temperature dependencies into the Preisach probability function, Eq. (5), we certainly simplify the picture accounting only that the system free-energy barriers should collapse as $T \to T_G$.

An effective medium approximation of metallic regions within a polaronic background having activated electrical conductivity was also intensively discussed earlier (see, e.g., Refs. 10, 39, 48, and 49). However, in those models the temperature- and field-dependent metallic-bond concentration was extracted from the resistivity data. In our approach, the magnitude of this mixing (value of the metal and polaron paths) is determined by the Preisach distribution function *without the need for empirical input from the magnetoresistive data*. Particularly, there is no need to introduce any secondary order parameter (see, e.g., Ref. 48) to reproduce the qualitative features of the experimental data.

As is mentioned in Sec. III, our approach implies that metallicity accompanies the establishment of an infinite percolating pathway, i.e., ferromagnetism precedes metallicity. The calculations confirm the percolation mechanism of conductivity. As is apparent form the data in Table I, the metal-to-insulator transition temperature T_{MI} is not larger than T_C but not less than T_B. The system blocking temperature lies between the two limits T_{BL} and T_{BH}, corresponding to excitation/blocking the lowest and the highest anisotropy barriers, respectively. Once the highest barrier hysterons freeze they are capable to keep *static* local magnetic order. But only when a static percolating ferromagnetic cluster is formed the metallicity establishes. However even below this temperature, the hysterons with lowest anisotropy energy, i.e., those with $T_{BL}<T_{BH}$, are in a superparamagnetic state and are not capable to keep static magnetic order and thus to support metallicity, as well. As far as for any system $T_{BL}<T_B<T_{BH}$,[32] and the relation $T_B \leq T_{MI} \leq T_C$ (see Table I) found, an immediate corollary is the percolating mechanism of metallicity. Still, at this stage of investigation, we cannot give definite answer to the question whether the Curie temperature coincides with the metal-to-insulator transition temperature or whether these two points are distinct.

Let us now consider the types of conductivity we attributed to hysterons. Theoretical predictions[6] state that in insulating phase $(d\rho/dT<0)$ electrons are bound by a surrounding lattice forming polaronic quasiparticles. Polaron hopping is the dominant transport mechanism here and give rise to the thermally activated resistivity. On cooling below T_{MI} spin order leads to electron delocalization and transition to metallic $(d\rho/dT>0)$ behavior.[6] Many experiments have provided compelling evidence for the existence of polaronic charge carriers in the paramagnetic state of manganites.[1–4] However, the electric transport mechanism below T_{MI} is still poorly understood. Although some experimental data are consistent with a polaron collapse at T_{MI}, other reports (see, e.g., Ref. 50 and references therein) provide evidence for the presence of polarons in the ferromagnetic metallic phase, as well. Within the framework of the phenomenological model proposed in this work, it is reasonable to attribute a polaronic type of conductivity to superparamagnetic hysterons. Then the existence of polarons below T_{MI} is naturally due to hysterons which remain in superparamagnetic state down to low temperatures far into the bulk ferromagnetic state. The prescription of the very same activation energy to polaronic quasiparticles above and below T_{MI} is definitely simplification which may be easily overcome. To avoid confusion, also note that keeping on the same magnitude of parameters in Eqs. (12) and (13) for systems with different $W_A(0)/W_{Cfl}$ ratio is a simplification, too.

As a final remark, note that there are a few features which should be kept in mind concerning the Griffiths-type phase in doped manganites. In the classic Griffiths model[26] exchange interaction is distributed randomly, but once distributed, it is fixed. This is not the case for doped manganites, where double-exchange coupling between Mn^{3+}-O^2-Mn^{4+} ions is due to electron hops between the ions and depends on mutual orientation of their core spins. As a consequence, as spins order locally, the ferromagnetic clusters are also more metallic, and the joint effect is to reinforce and stabilize the formation of large ferromagnetic clusters. Also, there is consensus between researchers that some fraction of ferromagnetic coupling between Mn ions is a superexchange type and so is in a nonmetallic regime. Hence, the situation in the doped manganites does not follow an ideal Griffiths phase precisely (see also discussion in Ref. 20). In this context, the ratio of characteristic energies $W_A(0)/W_{Cfl}$ should not be precisely considered as "the probability for the existence of a ferromagnetic bond." The parameter $W_A(0)/W_{Cfl}$ merely implements a role similar to the disorder parameter of the Griffiths model.

VI. SUMMARY

In the report, an effective medium approach is developed for clarifying the universal features in metal-insulator transition of the mixed-phase manganites. The formalism is based on generalization of the Preisach model of hysteresis for half-metallic ferromagnet and the assumption of the existence of Griffiths-type phase and temperature scale T_G above the magnetic-ordering temperature. Respectively, the fundamental characteristic energies which play a primary role in the metal-to-insulator transition and magnetoresistive properties of the system are determined by the energy barriers of similar to those of a hypothetical medium with the Curie temperature T_G. Within the model, the system is considered as three-dimensional random resistor network were the intrinsic thermodynamic percolation effects are not only due to magnetic field variation but also due to temperature changes, as well. The approach implies that the metallic state reached from the insulator with magnetic field increase is not homogenous but has a substantial fraction of semiconducting/insulating clusters, and the metallic clusters exist in the range $T_{MI} \leq T \leq T_G$. Accordingly, this also suggested that the metallic state reached from the insulator with temperature decrease is not homogeneous and even below T_{MI} there is a substantial fraction of the nonmetallic/paramagnetic clusters. Both mechanisms of percolation transition are considered on one basis. Within the approach, a natural parameter, that is, the ratio of two characteristic energies—the critical thermal-fluctuation energy and the zero-temperature anisotropy barrier—has been introduced for a qualitative classification of system magnetotransport properties. The model is able to describe the main experimental facts for doped manganites' resistivity on temperature and magnetic field dependencies without the need for empirical input from the magnetoresistive data.

ACKNOWLEDGMENTS

We thank D. C. Jiles and S. M. Ryabchenko for fruitful discussions. This research was supported by Cardiff University (Y.M.).

[1] J. M. Coey, M. Viret, and S. von Molnar, Adv. Phys. **48**, 167 (1999).
[2] M. B. Salamon and M. Jaime, Rev. Mod. Phys. **73**, 583 (2001).
[3] E. Dagotto, T. Hotta, and A. Moreo, Phys. Rep. **344**, 1 (2001).
[4] M. Ziese, Rep. Prog. Phys. **65**, 143 (2002).
[5] C. Zener, Phys. Rev. **81**, 440 (1951); P. W. Anderson and H. Hasegawa, *ibid.* **100**, 675 (1955); J. Goodenough, *ibid.* **100**, 564 (1955).
[6] A. J. Millis, P. B. Littlewood, and B. I. Shraiman, Phys. Rev. Lett. **74**, 5144 (1995); A. J. Millis, B. I. Shraiman, and R. Mueller, *ibid.* **77**, 175 (1996).
[7] J. Fontcuberta, B. Martinez, A. Seffar, S. Pinol, J. L. Garcia-Munoz, and X. Obradors, Phys. Rev. Lett. **76**, 1122 (1996).
[8] J. O'Donnell, M. Onellion, M. S. Rzchowski, J. N. Eckstein, and I. Bozovic, Phys. Rev. B **54**, R6841 (1996).
[9] M. Viret, L. Ranno, and J. M. D. Coey, Phys. Rev. B **55**, 8067 (1997).
[10] S. L. Yuan, Z. Y. Li, W. Y. Zhao, G. Li, Y. Jiang, X. Y. Zeng, Y. P. Yang, G. Q. Zhang, F. Tu, C. Q. Tang, and S. Z. Jin, Phys. Rev. B **63**, 172415 (2001).
[11] M. Fäth, S. Freisen, A. A. Menovsky, Y. Tomioka, J. Aarts, and J. A. Mydosh, Science **285**, 1540 (1999).
[12] R. D. Merithew, M. B. Weissman, F. M. Hess, P. Spradling, E. R. Nowak, J. O'Donnell, J. N. Eckstein, Y. Tokura, and Y. Tomioka, Phys. Rev. Lett. **84**, 3442 (2000).
[13] R. H. Heffner, J. E. Sonier, D. E. MacLaughlin, G. J. Nieuwenhuys, G. Ehlers, F. Mezei, S.-W. Cheong, J. S. Gardner, and H. Röder, Phys. Rev. Lett. **85**, 3285 (2000).
[14] P. Dai, J. A. Fernandez-Baca, N. Wakabayashi, E. W. Plummer, Y. Tomioka, and Y. Tokura, Phys. Rev. Lett. **85**, 2553 (2000); C. P. Adams, J. W. Lynn, Y. M. Mukovskii, A. A. Arsenov, and D. A. Shulyatev, *ibid.* **85**, 3954 (2000).
[15] J. M. D. Coey, M. Viret, L. Ranno, and K. Ounadjela, Phys. Rev. Lett. **75**, 3910 (1995).
[16] K. Khazeni, Y. X. Jia, Li Lu, V. H. Crespi, M. L. Cohen, and A. Zettl, Phys. Rev. Lett. **76**, 295 (1996).
[17] T. Okuda, Y. Tomioka, A. Asamitsu, and Y. Tokura, Phys. Rev. B **61**, 8009 (2000).
[18] Y. Tomioka, A. Asamitsu, and Y. Tokura, Phys. Rev. B **63**, 024421 (2000).
[19] M. B. Salamon, P. Lin, and S. H. Chun, Phys. Rev. Lett. **88**, 197203 (2002).
[20] M. B. Salamon and S. H. Chun, Phys. Rev. B **68**, 014411 (2003).
[21] D. Akahoshi, M. Uchida, Y. Tomioka, T. Arima, Y. Matsui, and Y. Tokura, Phys. Rev. Lett. **90**, 177203 (2003).
[22] V. M. Kalita, A. F. Lozenko, S. M. Ryabchenko, P. O. Trotsenko, O. I. Tovstolytkin, and A. M. Pogorily, Ukr. J. Phys. **54**, 157 (2009).
[23] J. Deisenhofer, D. Braak, H.-A. Krug von Nidda, J. Hemberger, R. M. Eremina, V. A. Ivanshin, A. M. Balbashov, G. Jug, A. Loidl, T. Kimura, and Y. Tokura, Phys. Rev. Lett. **95**, 257202 (2005).
[24] J. Burgy, A. Moreo, and E. Dagotto, Phys. Rev. Lett. **92**, 097202 (2004).
[25] P. Y. Chan, N. Goldenfeld, and M. Salamon, Phys. Rev. Lett. **97**, 137201 (2006).
[26] R. Griffiths, Phys. Rev. Lett. **23**, 17 (1969); A. J. Bray, *ibid.* **59**, 586 (1987).
[27] W. Jiang, X. Z. Zhou, G. Williams, R. Privezentsev, and Y. Mukovskii, Phys. Rev. B **79**, 214433 (2009).
[28] A. K. Pramanik and A. Banerjee, Phys. Rev. B **81**, 024431 (2010).
[29] V. N. Krivoruchko, Y. Melikhov, and D. C. Jiles, Phys. Rev. B **77**, 180406(R) (2008).
[30] F. Preisach, Z. Phys. **94**, 277 (1935).
[31] G. Bertotti, *Hysteresis in Magnetism* (Academic, New York, 1998).
[32] T. Song, R. M. Roshko, and E. Dan Dahlberg, J. Phys.: Condens. Matter **13**, 3443 (2001).
[33] V. Basso, C. Beatrice, M. LoBue, P. Tiberto, and G. Bertotti, Phys. Rev. B **61**, 1278 (2000).
[34] L. Neel, Ann. Geophys. (C.N.R.S.) **5**, 99 (1949).
[35] K. H. Ahn, T. Lookman, and A. R. Bishop, J. Appl. Phys. **99**, 08A703 (2006).
[36] If we take into account that the activation energy required for the carries hopping depends on magnetic field then this assumption is not correct, i.e., $\sigma_{rev}(T) \neq \sigma_{sp}(T,H)$.
[37] N. Panwar, A. Rao, R. S. Singh, W. K. Syu, N. Kaurav, Y.-K. Kuo, and S. K. Agarwal1, J. Appl. Phys. **104**, 083906 (2008).
[38] K. Kubo and N. Ohata, J. Phys. Soc. Jpn. **33**, 21 (1972).
[39] G. J. Snyder, C. H. Booth, F. Bridges, R. Hiskes, S. DiCarolis, M. R. Beasley, and T. H. Geballe, Phys. Rev. B **55**, 6453 (1997); V. N. Krivoruchko and S. I. Khartsev, Low Temp. Phys. **24**, 803 (1998); Y.-H. Huang, C.-S. Liao, Z.-M. Wang, X.-H. Li, C.-H. Yan, J.-R. Sun, and B.-G. Shen, Phys. Rev. B **65**, 184423 (2002); M. Viret, F. Ott, J. P. Renard, H. Glättli, L. Pinsard-Gaudart, and A. Revcolevschi, Phys. Rev. Lett. **93**, 217402 (2004).
[40] M. Jaime, H. T. Hardner, M. B. Salamon, M. Rubinstein, P. Dorsey, and D. Emin, Phys. Rev. Lett. **78**, 951 (1997).
[41] Y. Chen, B. G. Ueland, J. W. Lynn, G. L. Bychkov, S. N. Barilo, and Y. M. Mukovskii, Phys. Rev. B **78**, 212301 (2008).
[42] N. F. Mott and E. A. Davis, *Electronic Processes in Non-Crystalline Materials* (Clarendon, Oxford, 1979).
[43] Ya. M. Strelniker, R. Berkovits, A. Frydman, and S. Havlin, Phys. Rev. E **69**, 065105(R) (2004); S. Ju, K. W. Yu, and Z. Y. Li, Phys. Rev. B **71**, 224401 (2005); S. Ju, T.-Y. Cai, and Z. Y. Li, *ibid.* **72**, 184413 (2005).
[44] N. G. Bebenin and V. V. Ustinov, J. Phys.: Condens. Matter **10**, 6301 (1998).
[45] P. Wagner, I. Gordon, L. Trappeniers, J. Vanacken, F. Herlach, V. V. Moshchalkov, and Y. Bruynseraede, Phys. Rev. Lett. **81**, 3980 (1998).
[46] E. Della Torre, E. Pinzaglia, and E. Cardelli, Physica B **372**, 115 (2006); E. Cardelli, E. Della Torre, and A. Faba, J. Appl. Phys. **103**, 07D927 (2008).
[47] C. R. Pike, A. P. Roberts, and K. L. Verosub, J. Appl. Phys. **85**, 6660 (1999).
[48] M. Jaime, P. Lin, S. H. Chun, M. B. Salamon, P. Dorsey, and M. Rubinstein, Phys. Rev. B **60**, 1028 (1999).
[49] M. Mayr, A. Moreo, J. A. Vergés, J. Arispe, A. Feiguin, and E. Dagotto, Phys. Rev. Lett. **86**, 135 (2001).
[50] G.-M. Zhao, V. Smolyaninova, W. Prellier, and H. Keller, Phys. Rev. Lett. **84**, 6086 (2000); S. Seiro, Y. Fasano, I. Maggio-Aprile, E. Koller, O. Kuffer, and Ø. Fischer, Phys. Rev. B **77**, 020407(R) (2008).